JCTC Journal of Chemical Theory and Computation

Cholesky Decomposition-Based Multiconfiguration Second-Order Perturbation Theory (CD-CASPT2): Application to the Spin-State Energetics of Co^{III}(diiminato)(NPh)

Francesco Aquilante,[‡] Per-Åke Malmqvist,[‡] Thomas Bondo Pedersen,[†,‡] Abhik Ghosh,[§] and Björn Olof Roos*[,‡]

Department of Theoretical Chemistry, Chemical Center, University of Lund, P.O. Box 124, S-221 00 Lund, Sweden, and Department of Chemistry, University of Tromsø, N-9037 Tromsø, Norway

Received October 15, 2007

Abstract: The electronic structure and low-lying electronic states of a Co^{III}(diiminato)(NPh) complex have been studied using multiconfigurational wave function theory (CASSCF/CASPT2). The results have been compared to those obtained with density functional theory. The best agreement with ab initio results is obtained with a modified B3LYP functional containing a reduced amount (15%) of Hartree–Fock exchange. A relativistic basis set with 869 functions has been employed in the most extensive ab initio calculations, where a Cholesky decomposition technique was used to overcome problems arising from the large size of the two-electron integral matrix. It is shown that this approximation reproduces results obtained with the full integral set to a high accuracy, thus opening the possibility to use this approach to perform multiconfigurational wave-function-based quantum chemistry on much larger systems relative to what has been possible until now.

1. Introduction

Seen from an inorganic or bioinorganic vantage point, high-level ab initio methods are somewhat of a succès d'estime[1] (for reviews on inorganic and bioinorganic applications of the present type of ab initio calculations, see refs 2–4). By and large, applications of such methods have been limited to small systems that are of limited interest in inorganic and bioinorganic chemistry. Of course, this does not mean that these methods have not been useful at all. Thus, high-level ab initio calculations have been recently deployed to analyze the electronic structures of multiply bonded transition metal and actinide dimer complexes.[5] However, it is density functional theory (DFT) that, in spite of its limited accuracy, has emerged as the standard method for modeling complex processes involving transition metals such as metalloenzyme mechanisms.[6–9] The major reason underlying this state of affairs is of course that much more computational effort is required with the application of the wave-function-based ab initio methods. Limitations in terms of the number of atoms and the size of the basis sets are more severe than they are in DFT. However, the situation vis-à-vis ab initio methods is now changing with the development of much more efficient techniques to treat the basis set problem.

Here, we report an extension of multiconfiguration reference, second-order perturbation theory (CASSCF/CASPT2),[10–12] based on a Cholesky decomposition (CD) of the electron repulsion integral matrix,[13–16] which is considerably faster than earlier implementations of the same method. Application of the Cholesky decomposition approach to electronic structure calculations is not new,[17–21] but only very recently[22] has the approach been successfully extended to multiconfigurational wave function models, such as the popular CASSCF method.[10] The general applicability of the CASSCF

* Corresponding author e-mail: Bjorn.Roos@teokem.lu.se.

† Present address: Atomistix A/S, c/o Niels Bohr Institute, Rockefeller Complex, Juliane Maries Vej 30, DK-2100 Copenhagen, Denmark.

‡ University of Lund.

§ University of Tromsø.

10.1021/ct700263h CCC: $40.75
Published on Web 04/16/2008

wave function, combined with the accuracy of the CASPT2 correction, affords a unique protocol for unraveling the subtleties of chemical bonds in transition metal systems. The computational expediency afforded by the Cholesky decomposition approach should go a long way toward establishing the CASSCF/CASPT2 method as a valuable tool in the theoretical inorganic and bioinorganic chemist's toolbox.

The Cholesky decomposition-based CASPT2 (CD-CASPT2) method is illustrated here with calculations on the spin-state energetics of the low-coordinate imido complex Co^{III}(diiminato)(NPh). This complex may be regarded as a slightly simplified C_{2v} model of the closely related, diamagnetic complex Co^{III}(nacnac)(NAd) (nacnac = anion of 2,4-bis(2,6-dimethylphenylimido)pentane, Ad = 1-adamantyl), which has been synthesized and structurally characterized.[23] The diamagnetism of this species, which has been attributed to a $(3d_{z^2})^2(3d_{x^2-y^2})^2(3d_{xy})^2$ electronic configuration on the basis of DFT calculations (where the z direction is identified with the $Co-N_{imido}$ axis), is noteworthy in that the σ^* d_{z^2}-based molecular orbital (MO) is occupied preferentially, whereas the corresponding d_{xz}- and d_{yz}-based π^* MOs are left unoccupied.[24] A detailed DFT study,[24] including calculations on the corresponding oxo complex, showed that this electronic configuration may be attributed to both the low-coordinate nature of the metal center and the nature of the imido ligand. However, the DFT studies, where the newer OPTX-based functionals OLYP and OPBE appeared to be the most reliable,[25] also suggested that there should be low-lying paramagnetic excited states. Indeed, another $Co^{III}-$imido complex with an $S = 0$ ground state, Co^{III}-($Tp^{tBu,Me}$)(NAd) ($Tp^{tBu,Me}$ = hydrotris(3-*t*-butyl-5-methylpyrazol-1-yl)borate), has been found to exhibit spin-crossover behavior, as a result of the existence of one or more low-lying, paramagnetic excited states.[26,27] Once again, DFT calculations, especially the OLYP and OPBE functionals, appeared to nicely capture the experimental scenario.[28]

That said, the calculation of the spin-state energetics of open-shell transition metal complexes has long been recognized as a difficult problem for DFT.[4] No one functional appears to perform well for all the problematic cases. A number of studies comparing the performance of different functionals vis-à-vis transition metal spin-state energetics have underscored this problem.[29–40]

Accordingly, the calibration of DFT spin-state energetics against high-level ab initio methods is an important goal for current quantum chemistry method development efforts. In this study, we shall compare DFT and CASPT2 results on the vertical spin-state energetics of Co^{III}(diiminato)(NPh). We shall also use this model complex to calibrate the CD-CASPT2 method against the conventional, full integral-based calculations. Both the CD and conventional CASPT2 calculations were performed with a relativistic double-ζ plus polarization (VDZP) basis set, whereas our best results were obtained using a valence triple-ζ plus polarization (VTZP) basis set where only CD-CASPT2 calculations proved feasible. Given the methodological focus of this study, we will not provide a comprehensive list of references to the transition metal imido literature, but instead will refer the reader to a recent review and references therein.[41]

2. Methodology

The present study has been carried out in part using the Cholesky decomposition representation[13,15] of electron repulsion integrals in all stages of the calculations (integrals, self-consistent field (SCF), CASSCF, and CASPT2). A brief review of this approach is given below. Details of the calculations, the choice of basis set, the active orbitals, and so forth, are given below. For more details about the Cholesky decomposition techniques, see the references given.

2.1. Cholesky Representation of the Electron Repulsion Integrals. The computational complexity of the CASPT2 method[11] depends on two parameters: the size of the space spanned by the complete active space (CAS) reference function and the size of the atomic basis set. The former is determined by the choice of the active space and grows factorially with the size of the active space. At present, CASPT2 calculations are therefore restricted to active spaces of about 14–16 orbitals. Fortunately, it turns out that suitable active spaces can be devised even for extended systems, while ensuring a computationally feasible size of the resulting CAS expansion.

On the other hand, the convergence of the results with respect to the size of the atomic basis set can be slow, as in other ab initio methods. When large basis sets are employed, the computational bottleneck of the CASPT2 method lies in the transformation of electron repulsion integrals (ERIs) from an atomic orbital (AO) to an MO basis. Along with the final MO integrals, the AO integrals and all partially transformed integral intermediates are responsible for the significant storage demands of the CASPT2 method.

A strategy for avoiding the expensive MO transformation of the entire ERI matrix and the storage of the AO ERIs derives from the fact that $1/r_{12}$ is a positive definite operator with eigenvalues clustered toward zero. This property allows for a compact representation of the ERIs by means of an incomplete CD of the matrix. The Cholesky representation of AO electron repulsion integrals may be written as[13,15]

$$(\mu\nu|\lambda\sigma) = \sum_{J}^{M} L_{\mu\nu}^{J} L_{\lambda\sigma}^{J} \tag{1}$$

where Greek indices denote AOs and $L_{\mu\nu}^{J}$ is the Jth Cholesky vector obtained from the matrix decomposition. Due to near linear dependence in the product space of the AOs, the number of vectors M needed to numerically represent the integrals to an accuracy suited for quantum chemical calculations is significantly smaller than the full dimension of the integral matrix. For most applications, the CD usually needs to be converged to an accuracy (δ) no better than 10^{-4}, and the resulting value of M is only about 3–4 times the number of atomic orbital basis functions (N). Notwithstanding the very few applications since its first appearance,[14,42,43] the CD approach has gained interest in recent years as a possible means to speed up correlated calculations.[13,17–20,44]

Recasting the equations for the evaluation of Fock matrices and for the MO transformation of the ERIs directly in terms of Cholesky vectors results in an immediate reduction in the computational costs of most ab initio or DFT methods.[15–17] Simultaneously, there is also an enormous reduction in

storage demands compared to conventional integral calculations. For the standard choice of the CD threshold ($\delta = 10^{-4}$), the disk space required to store the AO basis Cholesky vectors is usually about 1–5% of the total size of the AO ERI matrix. The onset of input−output bottlenecks related to the manipulation of these arrays is therefore shifted to significantly larger atomic basis sets, when using the CD approximation. The implementation of the CD-CASPT2 method in this work aims at taking advantage of this particular aspect of the CD representation of the AO ERIs. The Fock matrix needed in CASPT2 can be computed from the AO Cholesky vectors in an efficient way by employing the recently proposed "local K" screening[16] of the exchange contributions.

A more demanding task is the generation of the right-hand side (RHS) of the equation system, which determines the excitation amplitudes. These are directly dependent on MO ERI elements of the type $(pi|qk)$, where p and q are either active or secondary orbitals, while i and k are either inactive or active orbitals. Frozen orbitals are of course excluded. First, transformed Cholesky vectors L^J_{pi} are computed. This task scales as ON^2M, where O is the number of inactive and active orbitals. Subsets of integrals are computed as

$$(pi|qk) = \sum_J^M L^J_{pi} L^J_{qk} \qquad (2)$$

and the resulting RHS elements are stored on disk. The assembly of the $(pi|qk)$ integrals scales as O^2V^2M, rather than the ON^4 required by a conventional MO transformation of the ERIs. The gain comes from the reduced prefactor ($O \ll N$), although the overall scaling is still fifth-order.

The present implementation is not yet optimal. The generation of the RHS elements requires an excessive amount of reading and writing to disk, and in spite of the out-of-core handling, a large amount of memory is needed. In future implementations, this part of the calculation will be more open-ended in the sense of requiring much less memory, and the amount of reading and writing will be reduced. We shall return to the subject of an optimal implementation of CD-CASPT2 in future publications. Nonetheless, we wish to stress that the present implementation, although of limited applicability to large systems, allows us to perform CASPT2 calculations that would be impossible with the conventional implementation. This is achieved because the CD method completely bypasses the AO ERIs' storage bottleneck and also because it produces the needed MO integrals at reduced computational costs and input−output overheads. In the present study, full CASSCF/CASPT2 calculations have been performed with a basis set consisting of 869 basis functions. The same CASSCF calculation is an order of magnitude faster in the Cholesky formulation. A more detailed account of the application of the present scheme to CASSCF wave functions has recently been given.[22]

2.2. Details of the Calculations. The Co^{III}(diiminato)-(NPh) model complex used in this study is depicted in Figure 1. The molecule is oriented such that the Co is at the origin, the imido nitrogen is on the z axis, and the phenylimido and 1,3-propanediiminato groups are in the xz plane. The planes

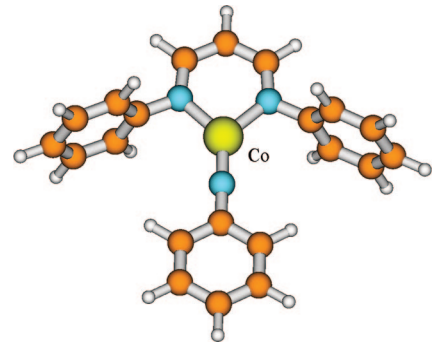

Figure 1. Model of the Co−imido complex used in the calculations.

of the terminal phenyl groups on the diiminato ligand are perpendicular to the plane of the remainder of the molecule. This 43-atom C_{2v} model complex may be viewed as a simplified version of the experimentally studied complex, Co^{III}(nacnac)(NAd).[23] The $S = 0$ ground state of the model complex was optimized with DFT (PW91 and OLYP/STO-TZP) using the ADF-2006 program system[45] and a Slater-type triple-ζ plus double polarization basis set. The structures so obtained were used in all additional DFT and CASSCF/CASPT2 calculations (which provided, in effect, vertical excitation energies). As detailed later, the Co−N_{imido} distance was also varied in some limited optimization studies at the CASPT2 level of theory.

Two different basis sets were employed in the CASSCF/CASPT2 calculations, both of which were generally contracted atomic natural orbital basis sets including scalar relativistic effects (ANO-RCC).[46,47] This implies that scalar relativistic effects are included at all levels of theory. The smaller one was of VDZP quality: Co/5s4p2d1f, N,C/3s2p1d, and H/2s. With this basis set, we performed calculations using both conventional integrals and the Cholesky approximation with two thresholds, $\delta = 10^{-4}$ and 10^{-8}. The overall basis set consists of 406 basis functions. The larger basis set was of VTZP quality (except for the hydrogens): Co/6s5p3d2f1g, N,C/4s3p2d1f, and H/2s1p. For this basis set, the total number of basis functions is 869. Only Cholesky-based calculations were performed with this basis set. With a threshold of $\delta = 10^{-4}$, it took 3.5 h (wall-clock time on a single AMD Opteron 148, 2.2 GHz, equipped with 1 GB of memory) to generate the Cholesky vectors. The corresponding time with the smaller basis set was 56 min, while the calculation of the full integral set took 151 min. A new method was used for the generation of starting orbitals for this set of calculations. An SCF calculation was performed, and subsequently, the occupied and virtual orbitals of each symmetry were separately localized using the recently developed Cholesky localization technique.[48] The localization, especially for the virtual orbitals, considerably simplified the selection of the physically appropriate orbitals for the active space.

Different active spaces were investigated for the CASSCF calculations, and the final choice was to include the five Co 3d orbitals and the two π orbitals (π_x and π_y) of the imido nitrogen in the active space. Three 4d orbitals were added to account for the "double shell" effect for the doubly

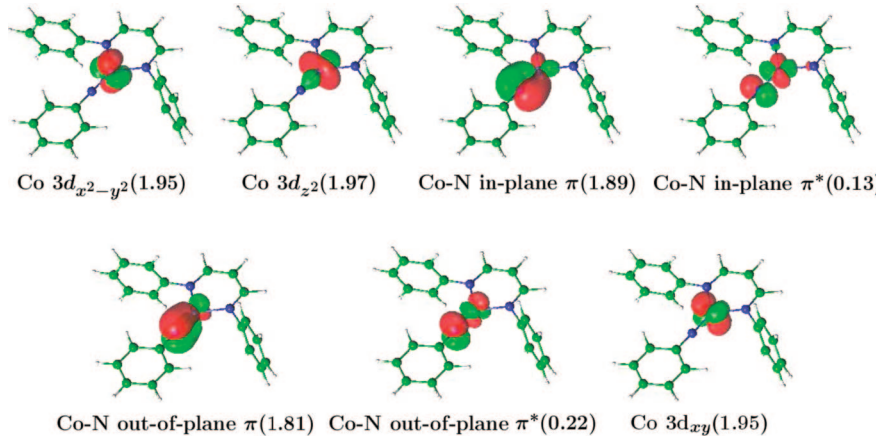

Figure 2. The active molecular orbitals in the Co^{III}(diiminato)(NPh) complex (except the 4d orbitals). A 0.05 au^{-3} level set surface was employed. Occupation numbers are shown in parentheses.

occupied 3d orbitals ($3d_{z^2}$, $3d_{yz}$, and $3d_{x^2-y^2}$).[49] This gives 10 active electrons in 10 orbitals (10in10). The CASSCF natural orbitals for the $^1A_1$ ground state are depicted in Figure 2 (the three weakly occupied 4d orbitals are not shown). Some test calculations were performed with a larger active space, which included also the lone-pair orbitals of the diiminato nitrogens. Their occupation numbers were, however, very close to two, which shows that they are not needed in the active space as long as the electronic states of interest do not involve charge-transfer excitations. Some of the calculations have been performed for a single root in each symmetry and spin. When more than one root was needed, state-average CASSCF calculations were performed.

All 132 valence electrons plus the Co 3s and 3p electrons were correlated in the CASPT2 calculations, which used the standard IPEA Hamiltonian and an imaginary level shift of 0.1 to remove some weak intruder states. The calculations were performed with the MOLCAS-7 quantum chemistry software.[50]

The chemical issue that we sought to address in this project concerns the spin-state energetics of the Co^{III}−imido complex; in other words, how much higher are the $S = 1$ and $S = 2$ states relative to the (experimentally observed) diamagnetic ground state? Accordingly, CASSCF/CASPT2 calculations were performed for the two lowest singlet, triplet, and quintet states in each of the four irreducible representations—in all, 24 electronic states. It turns out that they all have energies below 4 eV, relative to the $^1A_1$ ground state, and it is possible that additional low-lying states would have been found in this energy interval, had the number of roots been extended further. However, for purposes of determining several (∼10) of the lowest electronic states and for a comparison of CASPT2 and DFT energetics, we believe that we have calculated a sufficient number of electronic states.

Density functional calculations were performed for the first state in each symmetry and spin. In some cases, a second state was also computed by locking the number of occupied orbitals in each symmetry. These calculations were performed using a variety of exchange-correlation functionals and a Slater-type triple-ζ plus double polarization basis set. A C_{2v} symmetry constraint was used. The DFT calculations were performed with the ADF program.[45]

Table 1. The Lowest Excited Triplet and Quintet States in Co^{III}(diiminato)(NPh) (Energies in eV) Using a PW91 Ground-State Geometry

state	configuration	energy[a]
$^1A_1$	$(3d_{z^2})^2(3d_{x^2-y^2})^2(3d_{yz})^2(b_1)^2(b_2)^2$	
$^3B_2$	$3d_{x^2-y^2} \rightarrow b_2^*$	0.14(0.16)
$^3B_1$	$3d_{xy} \rightarrow b_2^*$	0.24(0.26)
$^5A_2$	$3d_{x^2-y^2}3d_{z^2} \rightarrow b_1^*b_2^*$	0.52(0.57)
$^5A_1$	$3d_{z^2}3d_{xy} \rightarrow (b_2^*)(b_2^*)$	0.60(0.65)
$^3A_2$	$3d_{z^2}3d_{xy} \rightarrow (b_2^*)^2$	1.11(1.19)
$^5B_1$	$3d_{x^2-y^2}3d_{xy} \rightarrow (b_1^*)(b_2^*)$	1.64(1.77)
$^5B_2$	$3d_{xy}b_2 \rightarrow b_1^*b_2^*$	1.85(1.99)
$^3A_1$	$b_2 \rightarrow (b_2^*)$	1.85(1.93)

[a] Energies obtained with a CASPT2 Co–N_{imido} optimized distance within parenthesis.

3. Results

We shall present two sets of results. First, we present the data obtained with the VDZP basis set where the Cholesky decomposition technique has not been used. Subsequently, we shall illustrate the use of the Cholesky technique and compare results obtained with the VDZP and VTZP basis sets. As we shall see, the two sets of results are very similar and most of the analysis can therefore be done at the VDZP level.

3.1. The Electronic Structure of Co^{III}(diiminato)(NPh). Here, we describe the different CASPT2 results obtained with the VDZP basis set. The calculations were first performed with a PW91 optimized geometry for the $^1A_1$ state, with a Co−imido distance of 1.653 Å. The 10in10 active space described above was used. CASPT2 calculations were performed for the lowest singlet, triplet, and quintet states in each symmetry. The seven strongly occupied active orbitals for the $^1A_1$ state are shown in Figure 2.

Vertical electronic excitation energies for the lowest triplet and quintet states in each symmetry are presented in Table 1, where we have used the following orbital labels: b_1 and b_1* are the "in-plane" Co−N_{imido} π orbitals and b_2 and b_2* are the "out-of-plane" Co−N_{imido} π orbitals. The CASPT2 calculations yield a closed-shell singlet as the ground state consistent with the observed diamagentism of Co^{III}(nacnac-)(NAd). There are, however, two low-lying triplet excited

Table 2. Vertical CASPT2/VDZP Energies (eV) of the Two Lowest Excited Singlet, Triplet, and Quintet States in Each Symmetry for Co^{III}(diiminato)(NPh) Using an OLYP Optimized Geometry for the Lowest Singlet State

state	configuration	energy[a]
1^1A_1	$(3d_{z^2})^2(3d_{x^2-y^2})^2(3d_{xy})^2(b_1)^2(b_2)^2$	
1^3B_2	$3d_{x^2-y^2} \rightarrow b_2^*$	0.11 (0.14)
1^3B_1	$3d_{xy} \rightarrow b_2^*$	0.15 (0.24)
2^3B_1	$3d_{z^2} \rightarrow b_1^*$	0.52
1^5A_1	$3d_{z^2}3d_{xy} \rightarrow b_1^*b_2^*$	0.59 (0.60)
1^5A_2	$3d_{x^2-y^2}3d_{z^2} \rightarrow b_1^*b_2^*$	0.59 (0.52)
2^3B_2	$3d_{xy} \rightarrow b_1^*$	0.65
1^1B_2	$3d_{x^2-y^2} \rightarrow b_2^*$	0.83
1^1B_1	$3d_{xy} \rightarrow b_2^*$	0.84 (0.84)
1^3A_1	$3d_{z^2}3d_{x^2-y^2} \rightarrow (b_2^*)^2$	0.96 (1.85)[b]
1^3A_2	$3d_{x^2-y^2}3d_{xy} \rightarrow (b_2^*)^2$	1.04 (1.11)
2^1B_2	$0.73(3d_{z^2} \rightarrow b_2^*) - 0.51(3d_{xy} \rightarrow b_1^*)$	1.07
2^3A_2	$3d_{z^2}3d_{x^2-y^2} \rightarrow b_1^*b_2^*$	1.35
2^3A_1	$3d_{z^2}3d_{xy} \rightarrow b_1^*b_2^*$	1.48
2^1B_1	$3d_{x^2-y^2} \rightarrow b_1^*$	1.52
2^5A_1	$3d_{x^2-y^2}3d_{xy} \rightarrow b_1^*b_2^*$	1.54
1^5B_1	$3d_{x^2-y^2}b_2 \rightarrow b_1^*b_2^*$	1.71 (1.64)
1^5B_2	$3d_{x^2-y^2}b_1 \rightarrow (b_1^*)(b_2^*)$	1.89 (1.85)
2^5B_2	$3d_{xy}b_2 \rightarrow b_1^*b_2^*$	1.91
2^5B_1	$3d_{xy}b_1 \rightarrow b_1^*b_2^*$	2.00
2^5A_2	$3d_{z^2}3d_{xy}b_1 \rightarrow b_1^*(b_2^*)^2$	2.56
1^1A_2	$b_1 \rightarrow b_2^*$	3.14
2^1A_1	$0.61(b_1 \rightarrow b_1^*) + 0.56(b_2 \rightarrow b_2^*)$	3.47
2^1A_2	$b_2 \rightarrow b_1^*$	3.90

[a] Values within parentheses are obtained using one root only. [b] Convergence to a different root (cf. Table 1).

states: $^3B_1$ at 0.24 eV and $^3B_2$ at 0.14 eV. A reoptimization of the geometries for these states may well change the relative ordering of the states. Moreover, the energy differences are so small that they are within the error limits of the CASPT2 method.

As previously discussed,[24] the electronic structure of the $^1A_1$ state is of unusual interest. There is a double bond between Co and the imido nitrogen consisting of two π-bonding orbitals, but there is no net $Co-N_{imido}$ σ bond, which is quite extraordinary. As may be seen from the natural orbital occupation numbers in Figure 2, the wave function is somewhat multiconfigurational, with occupation numbers for the antibonding orbitals of 0.13 and 0.22, respectively. The reason for the absence of a σ bond is the double occupancy of the $3d_{z^2}$ orbital, which is energetically more favorable than using it to form a σ bond. Moving electrons from this orbital to the b_1 or b_2 orbitals would enable the formation of a σ bond but at the expense of the π bonds. However, some of the low-lying excited states (cf. Table 2) have the $3d_{z^2}$ orbital singly occupied, resulting in a partial σ bond and less π bonding (e.g., the state 2^3B_1).

In order to study the energetics as a function of the $Co-N_{imido}$ distance, we reoptimized the latter at the CASPT2 level of theory. This led only to a modest change for the ground state: 1.632 Å (CASPT2) instead of 1.653 Å (PW91). The new excitation energies are given within parentheses in Table 1. They are slightly higher than those obtained with the DFT optimized bond distance. The calculations were then performed at the PW91 optimized geometry for the $^3B_2$ state, which has a $Co-N_{imido}$ bond distance of 1.70 Å. This led to the surprising result that the triplet energy, for which the geometry had been optimized with DFT, is higher than the triplet energy calculated at the singlet geometry. The closed-shell $^1A_1$ state is still the lowest state, and the excitation energies have not changed much. In order to study this problem in more detail, a set of calculations were performed where only the $Co-N_{imido}$ distance was varied, keeping all of the other geometry parameters at the singlet geometry. The results are shown in Figure 3 for the three states of lowest energy.

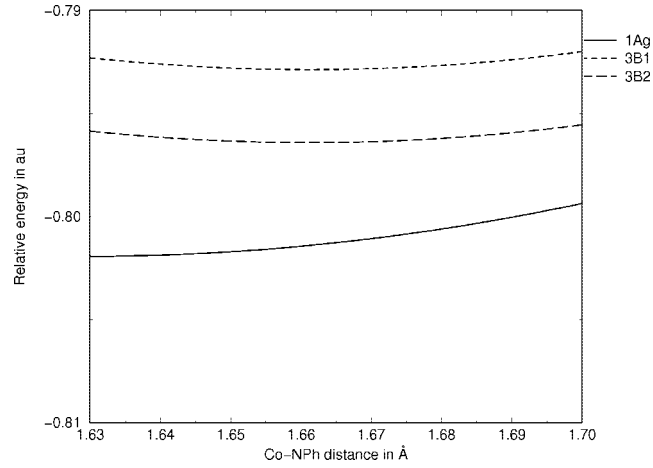

Figure 3. Energy of the three lowest states in the Co^{III}(diiminato)(NPh) complex as a function of the $Co-N_{imido}$ distance.

At the CASPT2/VDZP level, the ground state has a minimum at R(Co−N) = 1.632 Å; the next state, $^3B_1$, at 1.661 Å, is considerably shorter than the 1.70 Å of the DFT triplet geometry. The third state, $^3B_2$, has a minimum at the same distance. The three curves are almost parallel, indicating that the excitation energies are not very dependent on the geometry. Of course, this conclusion could change if other geometry parameters were also varied.

CASPT2 calculations were also performed using an OLYP optimized geometry, which is very similar to the one used above and has the same $Co-N_{imido}$ distance (1.653 Å). The results were very similar to those discussed above with one striking difference: the CASPT2 energy of 1.85 eV for the $^3A_1$ state with the PW91 ground-state geometry is now reduced to 0.99 eV (with the OLYP ground-state geometry). The reason for this is convergence to a different root in the CASSCF calculation, which is not surprising in view of the many near-degeneracies involved in this system. Depending on the starting geometry, two different calculations may therefore converge to different roots if they are close in energy. To explore the electronic structure in more detail, we therefore decided to extend the calculations to two roots in each symmetry. In total, 24 electronic states were computed (singlets, triplets, and quintets in each symmetry). The resulting energies are presented in Table 2.

The energies for the first root in each symmetry and spin are very similar to the energies presented in Table 1 with one exception. Comparing the two tables, we see that in one case the single root calculations have converged to the second state instead of the first. This can of course happen, especially when roots are as closely spaced as they are here. The other excitation energies are, however, very similar, and the wave

Table 3. Total CASPT2/VDZP Energies with and without the Cholesky Technique[a]

state	CASPT2	CD-CASPT2	energy difference
1^1A_1	−2364.79544388	−2364.79295568	−0.00248820
2^1A_1	−2364.67390089	−2364.67141410	−0.00248679
1^1B_1	−2364.77033932	−2364.76785555	−0.00248377
2^1B_1	−2364.74534751	−2364.74287943	−0.00246808
1^1B_2	−2364.77072043	−2364.76830977	−0.00241066
2^1B_2	−2364.76208911	−2364.75960783	−0.00248128
1^1A_2	−2364.68597422	−2364.68331489	−0.00265933
2^1A_2	−2364.65783067	−2364.69289360	0.03506293
1^3A_1	−2364.76595240	−2364.76355308	−0.00239932
2^3A_1	−2364.74697718	−2364.74449320	−0.00248398
1^3B_1	−2364.79568110	−2364.79317394	−0.00250716
2^3B_1	−2364.78222016	−2364.77976550	−0.00245466
1^3B_2	−2364.79732094	−2364.79489954	−0.00242140
2^3B_2	−2364.77725821	−2364.77474030	−0.00251791
1^3A_2	−2364.76313971	−2364.76067077	−0.00246894
2^3A_2	−2364.75177134	−2364.74936282	−0.00240852
1^5A_1	−2364.77946626	−2364.77696359	−0.00250267
2^5A_1	−2364.74481204	−2364.74236741	−0.00244463
1^5B_1	−2364.73843766	−2364.73598410	−0.00245356
2^5B_1	−2364.72771500	−2364.72518246	−0.00253254
1^5B_2	−2364.73200864	−2364.72953416	−0.00247448
2^5B_2	−2364.73100948	−2364.72850268	−0.00250680
1^5A_2	−2364.77947072	−2364.77704933	−0.00242139
2^5A_2	−2364.70713998	−2364.70466298	−0.00247700

[a] A threshold of 10^{-4} was used for the Cholesky decomposition.

functions have the same orbital occupancy. We can therefore limit ourselves to the two-root calculations in our further discussion.

Two triplet states have very low energies: $^3B_1$ and $^3B_2$. Their energies are so close to zero that we cannot conclusively determine the real ground state in this system. The accuracy of these calculations (or any other calculation) is certainly not better than 0.1 eV. Our results thus indicate that three electronic states are very close in energy, and they are all good candidates for the ground state. The density of states is very high: there are 20 electronic states below 2.0 eV. Several of these are doubly excited with respect to the $^1A_1$ ground state. The reason for this high density of states is that there are three doubly occupied 3d orbitals, which are very close in energy in the ground state: $3d_{z^2}$, $3d_{x^2-y^2}$, and $3d_{xy}$.

3.2. CD-CASPT2 Calculations. In this section, we shall study the effect of the basis set on the results obtained above. To perform calculations with a VTZP basis set (869 ANO-RCC functions), we needed to invoke the Cholesky decomposition technique. We started by calibrating this methodology against full integral calculations with the VDZP basis set used above. The results of this comparison are shown in Table 3, which gives the total CASPT2 energies obtained with and without CD. A threshold of 10^{-4} was used in decomposing the ERI matrix. The energy difference between the two sets of calculations is almost constant and on the order of 2×10^{-3} E_h (about 0.07 eV), which is an order of magnitude larger than the threshold used. More importantly, the relative energies of the states are affected by less than 0.01 eV. [There is one exception: the 2^1A_2 state, where the CD calculation converged to a different electronic state.] Calculations with a threshold of 10^{-8} gave absolute energies with an accuracy of about 10^{-6} au and relative energies identical to those obtained with full integrals. We therefore conclude that the CD calculations are accurate. On the basis of our earlier experience, we would expect the accuracy to be even better with the larger basis set.[22]

Table 4. Timing information for the Cholesky calculations[a]

	VDZP basis		
	conventional	Cholesky	VTZP basis
integrals	150	56	217
CASSCF/it[b]	4.25	0.41	3.88
CASPT2	383 (24)	163 (20)	898 (232)

[a] Wall times are given in minutes (CPU time within parentheses for the CASPT2 calculations). [b] Wall time per CASSCF iteration.

Table 5. A Comparison of the CASPT2 Relative Energies (eV) with the VDZP and VTZP Basis Sets

state	VTZP	VDZP	state	VTZP	VDZP
1^1A_1	0.00	0.00	2^3A_2	1.39	1.35
1^3B_1	0.02	0.15	2^1B_1	1.55	1.52
1^3B_2	0.18	0.11	2^5A_1	1.57	1.54
2^3B_1	0.59	0.52	1^5B_1	1.70	1.71
2^3B_2	0.63	0.65	1^5B_2	1.98	1.89
1^5A_1	0.63	0.59	2^3A_1	2.03	1.48[a]
1^5A_2	0.64	0.59	2^5B_1	2.40	2.00[a]
1^1B_2	0.86	0.83	2^5B_2	2.45	1.91[a]
1^1B_1	0.87	0.84	2^5A_2	2.59	2.56
1^3A_1	0.90	0.96	2^1A_2	2.82	3.90[a]
2^1B_2	1.04	1.07	1^1A_2	3.13	3.14
1^3A_2	1.05	1.04	2^1A_1	3.46	3.47

[a] Convergence to different roots.

Table 6. Relative Electronic Energies E_{rel}, Thermodynamic Energies (U_{rel}),[b] or Enthalpies (H_{rel})[c] and Relative Gibbs Free Energies G_{rel} Based on OLYP/STO-TZP Geometries and Harmonic Frequencies and the Ideal Gas Approximation at 298.15 K[a]

state	E_{rel}	U_{rel}/H_{rel}	G_{rel}
1^1A_1	0.00	0.00	0.00
1^3B_2	5.38(0.23)	4.96(0.21)	4.43(0.19)
1^3B_1	10.67(0.46)	10.17(0.44)	9.29(0.40)
2^3B_1	13.90(0.60)	11.78(0.51)	12.84(0.56)

[a] The energies shown are in kcal/mol (eV). [b] The thermodynamic energy U is the sum of the electronic energy E, the zero-point energy, and translational, vibrational, and rotational energies at 298.15 K. [c] Trends in U_{rel} and H_{rel} are identical since the work term RT in the latter cancels out.

Table 4 presents the wall-clock times obtained on an AMD Opteron 148 (2.2 GHz) PC for one single-root calculation ($^1A_1$). With the VDZP basis set, the generation of the Cholesky vectors is 3 times faster than the full integral calculation. The increase in speed is much larger for the VTZP basis set, where the calculation of the Cholesky vectors takes 217 min. The full integral calculation could not be performed in this case, but it may be estimated to be around 4500 min from the timing obtained for the VDZP basis set. In other words, the CD method results in a speedup by about a factor of 20. The overall CASSCF/VDZP calculations are a factor of 10 faster, a speedup that should also increase for the larger basis set. For the VTZP basis set, each CASSCF iteration takes 3.88 min, underscoring the effectiveness of the CD technique. The speedup of the CASPT2 calculations is less impressive. Not much is gained in CPU time, and I/O times overwhelmingly dominate the calculations. The reason for this was explained in the

Table 7. Comparison of Vertical Excitation Energies (eV) with CASPT2 and DFT

		CASPT2		DFT(STO-TZP)						
	electronic configuration	VDZP	VTZP	OLYP	OPBE	BLYP	PW91	BP86	B3LYP	B3LYP*
1^1A_1	$(3d_{z^2})^2(3d_{x^2-y^2})^2(3d_{xy})^2(b_1^*)^0(b_2^*)^0$	0.00	0.00	0.00	0.00	0.00	0.00	0.00	0.00	0.00
1^3B_2	$(3d_{z^2})^2(3d_{x^2-y^2})^1(3d_{xy})^2(b_1^*)^0(b_2^*)^1$	0.11	0.18	0.31	0.19	0.52	0.44	0.43	−0.09	0.07
1^3B_1	$(3d_{z^2})^2(3d_{x^2-y^2})^2(3d_{xy})^1(b_1^*)^0(b_2^*)^1$	0.15	0.02	0.60	0.55	0.70	0.67	0.66	0.06	0.23
2^3B_1	$(3d_{z^2})^2(3d_{x^2-y^2})^1(3d_{xy})^2(b_1^*)^1(b_2^*)^0$	0.52	0.59	0.88	0.82	1.08	1.04	1.03	0.24	0.51
2^3B_2	$(3d_{z^2})^2(3d_{x^2-y^2})^2(3d_{xy})^1(b_1^*)^1(b_2^*)^0$	0.65	0.63	1.35	1.31	1.50	1.46	1.45	0.54	0.83
1^5A_2	$(3d_{z^2})^1(3d_{x^2-y^2})^1(3d_{xy})^2(b_1^*)^1(b_2^*)^1$	0.59	0.64	1.01	0.84	1.47	1.35	1.34	0.33	0.63
1^5A_1	$(3d_{z^2})^2(3d_{x^2-y^2})^1(3d_{xy})^1(b_1^*)^1(b_2^*)^1$	0.59	0.63	1.19	1.06	1.63	1.53	1.51	0.47	0.77
max deviation[a]				0.72	0.68	0.87	0.90	0.88	0.35	0.21
rms deviation[a]				0.44	0.38	0.68	0.62	0.61	0.22	0.13

[a] Deviations from the CASPT2(VTZP) results.

Methodology section, and we expect that future versions of the MOLCAS program system will result in substantially improved timings. Nevertheless, we have demonstrated that a CASSCF/CASPT2 calculation with 869 ANO-RCC basis functions can be performed on a normal PC in less than 20 h of wall-clock time.

The results for the VTZP calculation are presented in Table 5 where they are compared with the VDZP results described above. Generally, the results are very similar. In a few cases the VTZP calculations of the second root converged to a different state, but we shall not study these cases here. They only mean that there are more low-lying states of the symmetry in question, and to obtain all of them correctly, one would have to increase the number of states included in the calculations. In most other cases, the energy differences are less than 0.1 eV with one exception. The 1^3B_1 state is now the second state and is virtually degenerate with the 1^1A_1 state. Remembering that the accuracy of the CASPT2 method is in general no better than about 0.2 eV, these results make it impossible to conclusively determine the ground state. All that can be concluded is that there are three candidates: 1^1A_1, 1^3B_1, and 1^3B_2.

3.3. Free Energy Differences. The question of definitively identifying the ground state cannot be addressed without including the zero-point energy and entropic effects. We have therefore computed these quantities for four of the lowest-energy states, using OLYP/STO-TZP geometries and harmonic frequencies and the ideal gas approximation at 298.15 K. The results are presented in Table 6. We note that these adiabatic relative energies are different from the vertical ones presented above. The changes, however, are small. Not surprisingly, geometry optimization lowers the energy of the triplet states, relative to the ground state, the margins being −0.04 eV for 1^3B_2, −0.06 eV for 1^3B_1, and −0.04 eV for 2^3B_1. Overall, according to Table 6, we still have at least two and possibly three near-degenerate lowest-energy states, and we cannot tell, on the basis of calculations alone, which should be the actual ground state.

4. Comparing CASPT2 and DFT

The CASPT2 results, which we estimate to be accurate to about ±0.2 eV, provide valuable calibration for DFT calculations of the energies of several of the low-lying spin states of Co^{III}(diiminato)(NPh). Seven low-lying states were calculated with seven popular exchange-correlation functionals at the OLYP, $S = 0$, ground-state geometry. Table 7 presents a comparison of the DFT/TZP and CASPT2 energetics. According to Table 7, the B3LYP* functional, which has a reduced amount (15%) of Hartree–Fock exchange relative to B3LYP (20%), appears to be in the best agreement with CASPT2. The more widely used B3LYP functional performs slightly worse, predicting (albeit by a margin of only 0.09 eV) a triplet $^3B_2$ ground state,[51] which is inconsistent with the experimentally observed diamagnetism of Co^{III}(nacnac)(NAd). In contrast, the classical pure functionals BLYP, PW91, and BP86 appear to exaggerate the instability of the higher-multiplicity states. The newer OPTX-based pure functionals[25] OLYP and OPBE are somewhat better in this respect. Between OLYP and OPBE, the energetics provided by OPBE appears to be in slightly better agreement with CASPT2 than those obtained with OLYP, as indicated by the slightly smaller root-mean-square (rms) error. The maximum deviations are, however, almost as large for these functionals as they are for the other pure functionals. In summary, among the functionals examined, B3LYP and in particular B3LYP* seem to be the only that are acceptable, as far as the spin-state energetics of Co^{III}-(diiminato)(NPh) are concerned. It will be interesting to see how well this conclusion might generalize as additional complexes are examined in similar studies. That said, there are many examples in the literature where B3LYP (or B3LYP*) has performed no better than and even distinctly worse than pure functionals.[29–40,52] The development of new, broadly applicable functionals is therefore very much an ongoing process.

5. Conclusions

This work, in our opinion, has contributed on three different fronts.

First, we have shown how CD of the two-electron integral matrix can be used to drastically simplify electronic structure calculations of large molecules and with accurate basis sets and wave-function-based methods. The CD method has been used in all stages of the calculations from SCF and CASSCF to CASPT2. The current implementation of this technique is not yet optimal but still allows calculations with nearly (and almost certainly somewhat over) 1000 basis functions. In the future, we expect to be able to use similarly accurate basis sets in ab initio studies of considerably larger molecules. Further improvement of the CD-CASPT2 part of our code[50] is needed for achieving this, but the technology is already at hand. The 43-atom molecule studied here was

treated with an ANO-RCC-VTZP basis set. With a Cholesky threshold of 10^{-4}, we can assume an accuracy better than 0.01 eV in the relative energies for 24 electronic states (this accuracy refers to the error introduced by the finite Cholesky function threshold). The generation of the Cholesky vectors with this threshold and the VTZP basis set is estimated to be about 20 times faster than the full generation of the ERI matrix. To this should be added the savings in disk storage requirement, which is reduced by several orders of magnitude. The large savings in computer time and resources combined with the maintained accuracy strongly suggest that the CD-CASPT2 approach will be the standard in future applications.

Second, CASPT2 calculations of the spin-state energetics of a Co^{III}(diiminato)(NPh) complex have provided valuable calibration of analogous DFT calculations. Surprisingly, such calibrations of DFT (vis-a-vis the specific issue of transition metal spin-state energetics) are quite rare. In this study, we have calculated seven low-lying spin states of Co^{III}(diiminato)(NPh) with seven common exchange-correlation functionals and compared the results with CASPT2. The B3LYP* functional, containing a reduced amount (15%) of exchange relative to the more widely used B3LYP functional, appears to be the best. Among the pure functionals examined, the newer OPTX-based functionals OPBE and OLYP appear to perform slightly better than older, classic functionals such as PW91, BLYP, and BP86 but still give unacceptably large rms error for the computed excitation energies.

Last, this study has also deepened our growing understanding of bonding in low-coordinate imido complexes. That all known Co^{III}−imido complexes exhibit diamagnetic ground states certainly appears to be a coincidence in light of the results obtained in this study. Thus, at least for Co^{III}−diiminato−imido complexes, our calculations predict multiple paramagnetic excited states at very low energies (perhaps as low as a couple of tenths of an electrovolt) above the ground state. This is an important facet of the electronic structure of these complexes that has not yet manifested itself in experimental studies.[23,28] However, as already mentioned, one or more thermally accessible paramagnetic excited states have been implicated for a hydrotrispyrazolylborate-supported Co^{III}−imido complex.[26–28]

Acknowledgment. This work has been supported by the Swedish Natural Science Research Council (VR) and by the Research Council of Norway. A.G. thanks Dr. Jeanet Conradie and Mr. Espen Tangen for assistance with the DFT calculations.

References

(1) Although translated tongue-in-cheek as a success that has run out of steam, this French expression is not a slur. Instead, it refers to a significant success that is appreciated by connoisseurs but lacks much of a popular following.

(2) Roos, B. O.; Andersson, K.; Fülscher, M. P.; Malmqvist, P.-Å.; Serrano-Andrés, L.; Pierloot, K.; Merchán, M. In *Advances in Chemical Physics: New Methods in Computational Quantum Mechanics*; Prigogine, I., Rice, S. A., Eds.; John Wiley & Sons: New York, 1996; Vol. XCIII, pp 219–332.

(3) Pierloot, K. *Mol. Phys.* **2003**, *101*, 2083–2094.

(4) Ghosh, A.; Taylor, P. R. *Curr. Opin. Chem. Biol.* **2003**, *91*, 113–124.

(5) Roos, B. O.; Borin, A. C.; Gagliardi, L. *Angew. Chem., Int. Ed.* **2006**, *46*, 1469–1472.

(6) Noodleman, L.; Lovell, T.; Han, W.-G.; Li, J.; Himo, F. *Chem. Rev.* **2004**, *104*, 459–508.

(7) Siegbahn, P. E. M.; Borowski, T. *Acc. Chem. Res.* **2006**, *39*, 729–738.

(8) Ghosh, A.; Steene, E. J. *Biol. Inorg. Chem.* **2001**, *6*, 739–752.

(9) Ghosh, A. *Acc. Chem. Res.* **2005**, *38*, 943–954.

(10) Roos, B. O. In *Advances in Chemical Physics; Ab Initio Methods in Quantum Chemistry - II*; Lawley, K. P., Ed.; John Wiley & Sons Ltd.: Chichester, England, 1987; chapter 69, p 399.

(11) Andersson, K.; Malmqvist, P.-Å.; Roos, B. O.; Sadlej, A. J.; Wolinski, K. J. *Phys. Chem.* **1990**, *94*, 5483–5488.

(12) Andersson, K.; Malmqvist, P.-Å.; Roos, B. O. *J. Chem. Phys.* **1992**, *96*, 1218–1226.

(13) Beebe, N. H. F.; Linderberg, J. *Int. J. Quantum Chem.* **1977**, *7*, 683–705.

(14) Røeggen, I. R.; Wisløff-Nielsen, E. *Chem. Phys. Lett.* **1986**, *132*, 154–160.

(15) Koch, H.; Sánchez de Merás, A.; Pedersen, T. B. *J. Chem. Phys.* **2003**, *118*, 9481–9484.

(16) Aquilante, F.; Pedersen, T. B.; Lindh, R. *J. Chem. Phys.* **2007**, *126*, Art. no. 194106.

(17) Pedersen, T. B.; Sánchez de Merás, A. M. J.; Koch, H. *J. Chem. Phys.* **2004**, *120*, 8887–8897.

(18) Pedersen, T. B.; Koch, H.; Boman, L.; Sánchez de Merás, A. M. *J. Chem. Phys. Lett.* **2004**, *393*, 319–326.

(19) García Cuesta, I.; Pedersen, T. B.; Koch, H.; Sánchez de Merás, A. *ChemPhysChem* **2006**, *7*, 2503–2507.

(20) Fernández, B.; Pedersen, T. B.; Sánchez de Merás, A.; Koch, H. *Chem. Phys. Lett.* **2007**, *441*, 332–335.

(21) Öhrn, A.; Aquilante, F. *Phys. Chem. Chem. Phys.* **2007**, *9*, 470–480.

(22) Aquilante, F.; Pedersen, T. B.; Roos, B. O.; Sánchez de Merás, A.; Koch, H. *J. Chem. Phys.*, **2007**, submitted.

(23) Dai, X.; Kapoor, P.; Warren, T. H. *J. Am. Chem. Soc.* **2004**, *126*, 4798–4799.

(24) Conradie, J.; Ghosh, A. *J. Chem. Theory Comput.* **2007**, *3*, 689–702.

(25) The OPTX exchange functional: Handy, N. C.; Cohen, A. *Mol. Phys.* **2001**, *99*, 403–412.

(26) Shay, D. T.; Yap, G. P. A.; Zakharov, L. N.; Rheingold, A. L.; Theopold, K. H. *Angew. Chem., Int. Ed.* **2005**, *44*, 1508–1510.

(27) Shay, D. T.; Yap, G. P. A.; Zakharov, L. N.; Rheingold, A. L.; Theopold, K. H. *Angew. Chem., Int. Ed.*, **2006**, *45*, 7870–7870. Corrigendum.

(28) Wasbotten, I. H.; Ghosh, A. *Inorg. Chem.* **2007**, *46*, 7890–7898.

(29) Reiher, M.; Salomon, O.; Hess, B. *Theor. Chem. Acc.* **2001**, *107*, 48–51.

(30) Swart, M.; Ehlers, A. W.; Lammertsma, K. *J. Phys. Chem. A* **2004**, *108*, 5479–5483.

(31) Swart, M.; Ehlers, A. W.; Lammertsma, K. *Mol. Phys.* **2004**, *102*, 2467–2474.

(32) Deeth, R. J.; Fey, N. *J. Comput. Chem.* **2004**, *25*, 1840–1848.

(33) Groenhof, A. R.; Swart, M.; Ehlers, A. W.; Lammertsma, K. *J. Phys. Chem. A* **2005**, *109*, 3411–3417.

(34) Daku, L. M. L.; Vargas, A.; Hauser, A.; Fouqueau, A.; Casida, M. E. *ChemPhysChem* **2005**, *6*, 1393–1410.

(35) Ganzenmuller, G.; Berkaine, N.; Fouqueau, A.; Casida, M. E.; Reiher, M. J. *J. Chem. Phys.* **2005**, *0122*, Art. No. 234321.

(36) De Angelis, F.; Jin, N.; Car, R.; Groves, J. T. *Inorg. Chem.* **2006**, *45*, 4268–4276.

(37) Vargas, A.; Zerara, M.; Krausz, E.; Hauser, A.; Daku, L. M. L. *J. Chem. Theory Comput.* **2006**, *2*, 1342–1359.

(38) Rong, C. Y.; Lian, S. X.; Yin, D. L.; Shen, B.; Zhong, A. G.; Bartolotti, L.; Liu, S. B. *J. Chem. Phys.* **2006**, *125*, Art. No. 174102.

(39) Strickland, N.; Harvey, J. N. *J. Phys. Chem. B* **2007**, *111*, 841–852.

(40) Conradie, J.; Ghosh, A. *J. Phys. Chem. B* **2007**, *111*, 12621–12624.

(41) Mehn, M. P.; Peters, J. C. *J. Inorg. Biochem.* **2006**, *100*, 634–643.

(42) O'Neal, D. W.; Simons, J. *Int. J. Quantum Chem.* **1989**, *36*, 673–688.

(43) Wilson, S. *Comput. Phys. Commun.* **1990**, *58*, 71–81.

(44) García Cuesta, I.; Pedersen, T. B.; Koch, H.; Sánchez de Merás, A. M. *J. Chem. Phys. Lett.* **2004**, *390*, 170–175.

(45) Velde, G. T.; Baerends, E. J.; Guerra, C. F.; Gisbergen, S. J. A. V.; Snijders, J. G.; Ziegler, T. *J. Comput. Chem.* **2001**, *22*, 931–967. The ADF program system was obtained from Scientific Computing and Modeling, Amsterdam (http://www.scm.com).

(46) Roos, B. O.; Lindh, R.; Malmqvist, P.-Å.; Veryazov, V.; Widmark, P.-O. *J. Phys. Chem. A* **2004**, *108*, 2851.

(47) Roos, B. O.; Lindh, R.; Malmqvist, P.-Å.; Veryazov, V.; Widmark, P.-O. *J. Phys. Chem. A* **2005**, *109*, 6575–6579.

(48) Aquilante, F.; Pedersen, T. B.; Koch, H.; Sánchez de Merás, A. *J. Chem. Phys.* **2006**, *125*, Art. no. 174101.

(49) Andersson, K.; Roos, B. O. *Chem. Phys. Lett.* **1992**, *191*, 507.

(50) Karlström, G.; Lindh, R.; Malmqvist, P.-Å.; Roos, B. O.; Ryde, U.; Veryazov, V.; Widmark, P.-O.; Cossi, M.; Schimmelpfennig, B.; Neogrady, P.; Seijo, L. *Comp. Mater. Sci.* **2003**, *28*, 222–239.

(51) It should be mentioned that, if the same DFT/B3LYP calculations are performed using the ANO-RCC-VDZP basis set, including scalar relativistic effects, the 1^3B_2 state will appear 0.10 eV below the $^1A_1$ ground state. The energy difference for the 1^3B_1 state is +0.03 eV.

(52) Sorkin, A.; Iron, M. A.; Truhlar, D. G. *J. Chem. Theory Comput.* **2008**, *4*, 307–315.

CT700263H